Hybrid GRU-TCN Deep Learning with SELU Activation for Solar Irradiance and Photovoltaic Power Forecasting

Jihoon Moon *

Posted Date: 9 December 2024

doi: 10.20944/preprints202412.0711.v1

Keywords: GRU-TCN hybrid model; SELU activation function; solar irradiance forecasting; photovoltaic power prediction; deep learning methodologies; renewable energy systems

 doi:10.20944/preprints202412.0711.v1

Article

Hybrid GRU-TCN Deep Learning with SELU Activation for Solar Irradiance and Photovoltaic Power Forecasting

Jihoon Moon

Department of AI and Big Data, Soonchunhyang University, Asan 31538, Republic of Korea; jmoon22@sch.ac.kr

Abstract: Accurate forecasting of solar irradiance and photovoltaic (PV) power generation is critical for optimizing renewable energy integration and enhancing energy management systems. This study addresses the dual prediction of solar irradiance and PV power generation by developing a hybrid deep learning model that combines gated recurrent unit (GRU) and temporal convolutional network (TCN) along with scaled exponential linear unit (SELU) activation functions. The proposed GRU-TCN-SELU model leverages the strengths of GRUs in capturing temporal dependencies and TCNs in handling long-range patterns, while SELU activation ensures self-normalizing properties that enhance model convergence and performance. The model was trained and evaluated using datasets from Jeju Island, South Korea, and Alice Springs, Australia, encompassing various meteorological variables and historical solar data. Experimental results demonstrate that the GRU-TCN-SELU model outperforms traditional single-model approaches in terms of mean absolute error (MAE) and root mean square error (RMSE), achieving higher accuracy in both solar irradiance and PV power forecasts. These findings highlight the effectiveness of integrating GRU and TCN architectures with SELU activation for reliable renewable energy prediction, facilitating improved energy generation planning and smart energy management systems.

Keywords: GRU-TCN hybrid model; SELU activation function; solar irradiance forecasting; photovoltaic power prediction; deep learning methodologies; renewable energy systems

1. Introduction

As modern urban environments evolve into "smart cities," the integration of data-driven insights into renewable energy forecasting, photovoltaic power optimization, and sustainable infrastructure planning becomes a critical priority, without diminishing the importance of advancements in transportation management and resource allocation. Initial research efforts in this domain focused on enhancing pedestrian safety, as studies demonstrated the feasibility of vision-based analytics for identifying potential pedestrian risks at unsignalized crosswalks [1]. Building on such foundational work, multi-dimensional analytical frameworks—such as the use of online analytical processing (OLAP) with data cubes—have systematically uncovered intricate behavioral patterns, enabling the proactive assessment of pedestrian risk scenarios [2]. As the complexity of urban data increased, automated object behavioral feature extraction techniques refined risk detection processes, paving the way for more accurate and granular safety assessments [3].

The advent of deep learning (DL) models marked a significant turning point, offering robust capabilities for risk estimation and prediction. Advanced DL-based approaches enhanced the accuracy of urban traffic accident risk estimation [4], while edge-vision systems enabled real-time vehicle–pedestrian risk prediction and timely alerts [5]. The evaluation of strengthened school zone policies provided evidence-based insights into their effectiveness in improving pedestrian safety [6]. Beyond pedestrian-focused contexts, integrating visual and community environmental factors further improved motorcycle crash and casualty estimation models, broadening the applicability of data-driven safety interventions [7]. Simultaneously, novel trajectory collection and reconstruction methods

 doi:10.20944/preprints202412.0711.v1

advanced urban surveillance, ensuring more reliable behavioral data for safety analyses [8]. Understanding infrastructural influences on walkability also became critical, as crosswalk delays and zoning patterns were found to significantly shape pedestrian access [9].

As research progressed, DL approaches transitioned from mere accident prediction to proactive prevention strategies that emphasize early intervention [10]. Innovations such as asymmetric long-term graph multi-attention networks captured complex spatiotemporal dynamics, enabling long-range traffic speed forecasting [11]. Integrating data cube structures with predictive models refined collision risk estimation between vehicles and pedestrians [12], advanced our understanding of interactive behaviors at unsignalized crosswalks [13], and facilitated predictive collision risk area estimation [14]. Complementary methods, including vision-based object recognition [15] and human movement classification using acceleration data [16], further exemplified DL's versatility in interpreting heterogeneous urban mobility scenarios.

The adaptability of DL methodologies also extended into sustainable urban development endeavors. Stacking deep transfer learning approaches improved short-term building energy predictions under varied seasonalities and occupant schedules [17]. Researchers employed optimization techniques to select energy-efficient building materials suited to different climates [18], while three-dimensional mapping data extraction contributed to informed urban planning [19]. Employing data cube analysis and association rule mining unveiled complex energy consumption patterns in commercial buildings, guiding strategic energy management decisions [20]. Beyond built environments, the breadth of DL applications encompassed diverse contexts, including stress detection in animal populations [21], underscoring the robust, cross-domain capabilities of these frameworks.

Refinement of vision-based analytics continued, enabling more detailed assessments of potential pedestrian risks under varying conditions [22]. Emerging transportation paradigms, such as urban air mobility (UAM), also benefited from DL, which offered computationally efficient, vision-based methods for in-flight risky behavior recognition [23]. Meanwhile, advanced sensor-based modeling, such as estimating vehicle cuboids from monovision, highlighted DL's capacity to handle complex three-dimensional and geometric data challenges in real-world environments [24]. Building on these capabilities, the focus shifts to leveraging deep learning for critical sustainability applications, particularly in renewable energy systems where accurate forecasting of solar resources is paramount for the stability and efficiency of smart city infrastructures.

Amidst these multifaceted applications, one critical aspect of smart city sustainability is the reliable integration of renewable energy. Solar energy, given its environmental benefits and resource abundance, is central to achieving energy resilience. Yet, forecasting solar irradiance and photovoltaic (PV) power generation remains inherently challenging due to the nonlinear dependencies, long-range temporal patterns, and sensitivity to diverse meteorological factors. Previous work, including the introduction of self-attention-based DL models, has demonstrated improved PV forecasting accuracy [25]. However, to capitalize fully on these gains and support stable grid operations, there is a need for hybrid models that jointly harness the strengths of different DL architectures and stabilization techniques.

This study addresses this gap by proposing a hybrid deep learning model that integrates gated recurrent units (GRUs) and temporal convolutional networks (TCNs) with the scaled exponential linear unit (SELU) activation function. The proposed GRU-TCN-SELU framework makes three key contributions:

- We enhance predictive accuracy for solar irradiance and PV power forecasting by effectively capturing nonlinear dependencies and long-range temporal patterns, building on the challenges and opportunities identified in prior forecasting models.
- We improve model robustness and stability under diverse meteorological conditions through the integration of advanced activation functions, as previously highlighted as a critical requirement for reliable renewable energy systems in smart cities.
- We provide a scalable solution that supports seamless integration into broader smart city infrastructures, bridging the gap between renewable energy forecasting and sustainable urban development goals.

 doi:10.20944/preprints202412.0711.v1

By leveraging insights from prior research across urban safety, energy management, mobility behavior, and advanced data analytics, this research contributes a robust, scalable tool for optimizing renewable energy integration within smart cities, aligning data-driven analysis with the overarching goal of sustainable and intelligent urban development.

The remainder of this paper is organized as follows: Section 2 reviews related work on renewable energy forecasting. Section 3 describes the proposed GRU-TCN model and data preprocessing methods. Section 4 presents the experimental setup, results, and comparisons with benchmarks. Finally, Section 5 summarizes key findings and outlines future research directions.

2. Related Work

In the context of smart cities, accurate energy forecasting underpins strategic decision-making and resource optimization, making it essential for both energy suppliers and consumers to anticipate future demand patterns. Early research primarily focused on building-level electricity consumption forecasting using ensemble learning models, emphasizing the enhancement of predictive accuracy and the incorporation of explainable artificial intelligence (XAI) techniques to elucidate feature contributions [26–28]. For instance, methods based on decision trees and gradient boosting algorithms enabled the development of interpretable forecasting pipelines, while techniques such as online learning and dynamic feature selection enhanced model adaptability to non-stationary consumption trends [29–35]. These advancements have significantly informed the development of scalable short-term load forecasting (STLF) frameworks, which achieve an optimal balance between computational efficiency, model transparency, and deployment feasibility in dynamic smart city environments [36–38].

As forecasting requirements became more intricate, researchers explored techniques to manage data volatility, impute missing values, and accommodate variable building usage patterns. Machine learning (ML) approaches increasingly incorporated behavioral analytics and online learning paradigms, enabling models to adapt dynamically to non-stationary environments [39]. Data augmentation techniques and hybrid modeling strategies—combining ensemble ML methods with DL components—offered solutions to challenges such as limited training data, cold-start scenarios, and mid-term forecasting uncertainties, enhancing model robustness and predictive precision [40–46]. At the same time, DL architectures such as recurrent neural networks (RNNs) and convolutional neural networks (CNNs) excelled in capturing intricate temporal dependencies in energy data. Advanced variants, including GRUs, long short-term memory (LSTM) networks, and bidirectional LSTMs (Bi-LSTMs), further improved short- and mid-term load forecasting by uncovering long-range consumption patterns and correlations [47,48].

This evolution naturally extended to renewable energy forecasting, where accurate solar irradiance and PV generation predictions are crucial for integrating clean energy sources into smart city infrastructures. Researchers increasingly employed ensemble machine learning models and DL architectures to enhance the accuracy and interpretability of solar irradiance forecasts, integrating XAI tools to demystify model decision-making processes [49–52]. Advances in DL, such as transformer-based architectures and sophisticated optimization algorithms, addressed the complexities of multi-step-ahead PV forecasting by capturing nonlinear, multi-scale dependencies in meteorological and historical energy generation datasets [53,54]. Additionally, hybrid frameworks combining convolutional layers, attention mechanisms, and generative models improved model generalization and robustness, offering scalable, data-driven solutions for solar energy management that can be applied from individual buildings to regional energy networks [39,55,56].

Despite these advancements, existing approaches often fall short of simultaneously capturing intricate temporal dependencies, adapting to highly volatile conditions, ensuring model stability, and maintaining interpretability for stakeholders. To address these limitations, our study proposes a hybrid DL framework that combines GRUs and TCNs with SELU activation functions. This approach leverages the complementary strengths of advanced ML and DL techniques, prioritizing both model interpretability and computational efficiency. By tackling the limitations of previous methods, the proposed framework aims to deliver more resilient and accurate solar irradiance and PV power

 doi:10.20944/preprints202412.0711.v1

forecasting solutions, tailored to meet the dynamic and scalable requirements of smart city infrastructures.

3. Materials and Methods

3.1. Data Sources and Study Sites

This study integrates datasets from two distinct regions to develop and evaluate robust forecasting models for both solar irradiance and PV power generation.

The first dataset, obtained from the Korea Meteorological Administration (KMA), pertains to Jeju Island, South Korea—an area actively transitioning into a "smart island" by reducing reliance on conventional fossil fuels and expanding renewable energy systems (RESs). Specifically, data were collected from two key regions, Ildo-1 dong and Gosan-ri, which are central to Jeju's renewable energy initiatives [50,55]. The Jeju dataset spans eight years (2011–2018) and includes hourly meteorological and solar irradiance measurements recorded between 8 a.m. and 6 p.m., such as temperature, humidity, wind speed, sky condition, solar irradiance, and additional factors like soil temperature, total cloud volume, and sunshine amount. However, the analysis focuses on sky condition, temperature, humidity, and wind speed, aligning with KMA's short-term weather forecasts, as illustrated in Figure 1.

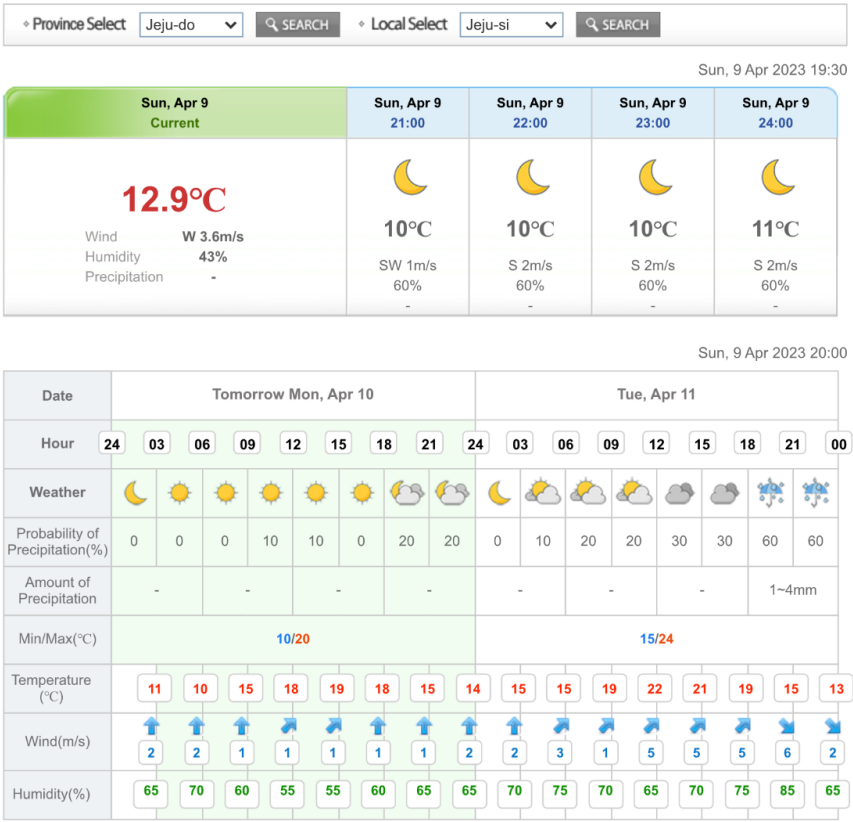

Figure 1. Meteorological data from KMA's short-term weather forecasts, including temperature, wind speed, humidity, and precipitation probabilities for Jeju Island.

The second dataset, acquired from the Desert Knowledge Australia Solar Center (DKASC) in Alice Springs, Australia [57], features hourly PV output data and meteorological variables essential for solar energy analysis. Data were collected over three years (2016–2019) and include timestamped records of wind speed, temperature, relative humidity, various radiation measures (e.g., global horizontal radiation, diffuse horizontal radiation, global tilted radiation, and diffuse tilted radiation), wind direction, daily rainfall, active energy delivered and received, current phase average, and active power. This dataset provides valuable insights into the performance of PV systems under the extreme arid climate conditions of Alice Springs. The inclusion of this dataset alongside the Jeju dataset allows for

 doi:10.20944/preprints202412.0711.v1

cross-regional model validation, emphasizing the scalability and robustness of forecasting techniques. Details of the DKASC dataset variables are summarized in Table 1.

Table 1. Meteorological and photovoltaic power data variables collected from the DKASC dataset.

No.	Columns
1	Timestamp
2	Wind Speed
3	Weather Temperature Celsius
4	Weather Relative Humidity
5	Global Horizontal Radiation
6	Diffuse Horizontal Radiation
7	Wind Direction
8	Weather Daily Rainfall
9	Radiation Global Tilted
10	Radiation Diffuse Tilted
11	Active Energy Delivered Received
12	Current Phase Average
13	Active Power

3.2. Data Preprocessing and Feature Engineering

3.2.1. Solar Irradiance

In this study, we addressed the issue of needing more data in the meteorological information collected for the KMA Jeju solar irradiance dataset. Approximately 0.1% of the total data for each category, including temperature, humidity, wind speed, and solar irradiation, were missing, with these missing values indicated as −1. We employed linear interpolation to estimate these missing values given their continuous data characteristics. For sky condition data, which were presented as categorical values from 1 to 4 (representing clear, partly cloudy, mostly cloudy, and cloudy), logistic regression was used to approximate missing values based on similarity with adjacent data.

To effectively reflect the periodicity of the date and maintain consistency with our previous study [55], we performed a day-ahead hourly solar irradiance forecasting using the same independent variables as shown in Table 2. The date information was first converted to Julian dates, ranging from 1 to 365 for common years or 366 for leap years, where January 1 corresponds to 1 and December 31 corresponds to 365 or 366. Subsequently, the one-dimensional date data were augmented into two-dimensional continuous data following Equations (1) and (2):

$$Date_x = \sin(360° \times Julian\ Date/365 \text{ or } 366), \quad (1)$$

$$Date_y = \cos(360° \times Julian\ Date/365 \text{ or } 366), \quad (2)$$

The sky condition variable comprised four categories on an interval scale from 1 to 4: clear, partly cloudy, mostly cloudy, and cloudy. The cloud amount was further represented by eleven scales according to the climatology 1/10 method used by the KMA. To effectively represent these categorical data, one-hot encoding was employed, assigning a value of 1 to the binary variable for a specific sky condition and 0 to all others. Similarly, one-hot encoding was applied to represent the hour factor, ranging from 8 a.m. to 6 p.m., as solar irradiance typically peaks between 12 p.m. and 2 p.m.

To account for recent trends in solar irradiance, we incorporated lagged meteorological variables from one day prior to the prediction time, including sky condition, temperature, humidity, wind speed, and solar irradiance, as independent variables. Consequently, the hybrid DL model construction dataset comprised 30 independent variables, with solar irradiance as the dependent variable. This comprehensive preprocessing pipeline, including sky conditions, time intervals, and recent weather trends, allowed for more accurate and adaptable predictions of intermittent solar irradiance in the KMA Jeju solar irradiance dataset.

Preprints.org (www.preprints.org) | NOT PEER-REVIEWED | Posted: 9 December 2024 doi:10.20944/preprints202412.0711.v1

Table 2. Comprehensive list of input variables (IVs) for day-ahead solar irradiance forecasting.

IV #	Description (Data Type)	IV #	Description (Data Type)
$Date_x$	$Date_x$ (continuous)	*W3*	*Mostly cloudy* (binary)
$Date_y$	$Date_y$ (continuous)	*W4*	*Cloudy* (binary)
T8	*8 a.m.* (binary)	*Temp*	*Temperature* (continuous)
T9	*9 a.m.* (binary)	*Humi*	*Humidity* (continuous)
T10	*10 a.m.* (binary)	*WS*	*Wind* speed (continuous)
T11	*11 a.m.* (binary)	$D1_{Day\_sin}$	$Date_{x,D-1}$ (continuous)
T12	*12 p.m.* (binary)	$D1_{Day\_cos}$	$Date_{y,D-1}$ (continuous)
T13	*1 p.m.* (binary)	$D1_{W1}$	$Clear_{D-1}$ (binary)
T14	*2 p.m.* (binary)	$D1_{W2}$	*Partly cloudy*$_{D-1}$ (binary)
T15	*3 p.m.* (binary)	$D1_{W3}$	*Mostly cloudy*$_{D-1}$ (binary)
T16	*4 p.m.* (binary)	$D1_{W4}$	*Cloudy*$_{D-1}$ (binary)
T17	*5 p.m.* (binary)	$D1_{Temp}$	*Temperature*$_{D-1}$ (continuous)
T18	*6 p.m.* (binary)	$D1_{Humi}$	*Humidity*$_{D-1}$ (continuous)
W1	*Clear* (binary)	$D1_{WS}$	*Wind speed*$_{D-1}$ (continuous)
W2	*Partly cloudy* (binary)	$D1_{Solar}$	*Solar irradiance*$_{D-1}$ (continuous)

3.2.2. Photovoltaic Power Generation

Because solar irradiance, the primary energy source for solar PV power, is highly dependent on time and weather, it is crucial to effectively incorporate external environmental data in forecasting models. Traditional date and time formats, however, are sequential, making it challenging to capture periodic relationships. For example, while 11 p.m. and midnight are adjacent in time, their numerical representation creates an artificial gap. To better address this periodicity, the DKASC dataset from Alice Springs was processed, as applied earlier to the KMA Jeju solar irradiance dataset, by transforming one-dimensional temporal data into two-dimensional representations using Equations (3)–(8):

$$Month_x = \sin(Month \times 2\pi/12), \quad (3)$$

$$Month_y = \cos(Month \times 2\pi/12), \quad (4)$$

$$Date_x = \sin(Day \times 2\pi/DOTM), \quad (5)$$

$$Date_y = \cos(Day \times 2\pi/DOTM), \quad (6)$$

$$Hour_x = \sin(Hour \times 2\pi/24), \quad (7)$$

$$Hour_y = \cos(Hour \times 2\pi/24), \quad (8)$$

where *DOTM* refers to the number of days in the respective month, which varies across February (28 or 29 days), March (31 days), and April (30 days), among others. This transformation ensures that periodic temporal relationships are accurately reflected in the model, similar to how they were represented in the **KMA Jeju solar irradiance dataset,** allowing for more effective representation of both short-term and long-term trends in solar irradiance and PV power generation.

Figure 2 presents a heat map visualization of the correlation between input variables and active power for the DKASC dataset. For the Sanyo panel data, solar irradiance exhibited a strong positive correlation with active power, reinforcing its critical role in PV forecasting. Conversely, variables such as wind direction, daily precipitation, and active energy supply displayed negligible correlations with active power and were thus excluded from the final feature set.

Preprints.org (www.preprints.org) | NOT PEER-REVIEWED | Posted: 9 December 2024 doi:10.20944/preprints202412.0711.v1

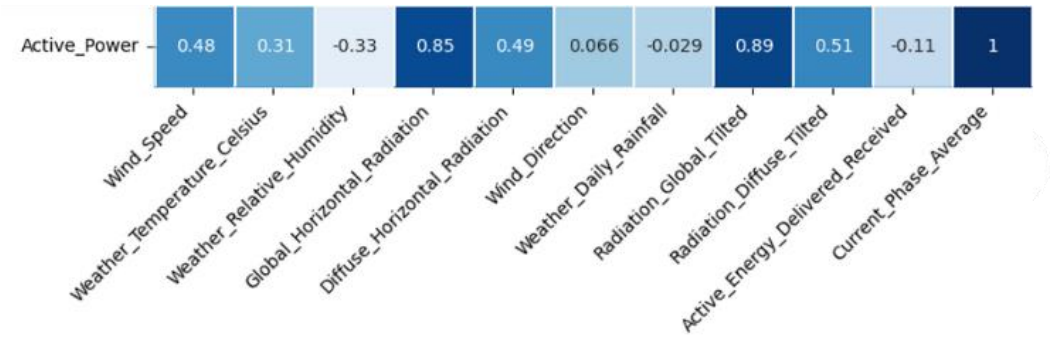

Figure 2. Correlation between input variables and active power in the DKASC dataset.

The DKASC dataset contained missing meteorological observations due to maintenance or equipment failures, leading to a total of 22,065 missing entries for wind speed and 971 missing entries for slope and scattered solar irradiance. Given the significant proportion of missing data, the wind speed variable was excluded from the analysis. In contrast, missing values for slope and scattered solar irradiance were addressed using linear interpolation, as applied earlier to the KMA Jeju solar irradiance dataset, ensuring data continuity.

Furthermore, all continuous variables were subjected to min-max normalization to account for differences in solar panel capacity and meteorological conditions, standardizing the range between 0 and 1 for training. By adopting the preprocessing methods previously applied to the KMA Jeju solar irradiance dataset, the DKASC dataset was prepared to reflect temporal periodicity, mitigate missing data challenges, and standardize variable magnitudes, ensuring consistency and robustness in the hybrid forecasting model across diverse meteorological contexts.

3.3. Data Preprocessing and Feature Engineering

This study proposes a hybrid DL model that integrates GRUs, TCNs, and self-attention mechanisms to accurately forecast solar irradiance in Jeju Island, South Korea, and PV power generation in Alice Springs, Australia. The sequence-to-sequence architecture leverages GRUs to capture short-term temporal dependencies and TCNs to identify long-range temporal patterns and nonlinear relationships in weather parameters. The addition of a self-attention mechanism further enhances the model's ability to focus on critical features and time steps, effectively addressing challenges such as nonlinear dependencies, sensitivity to meteorological factors, and long-term sequence modeling. This robust framework provides accurate and reliable forecasts for renewable energy systems in diverse environmental contexts. The complete model architecture is illustrated in Figure 3.

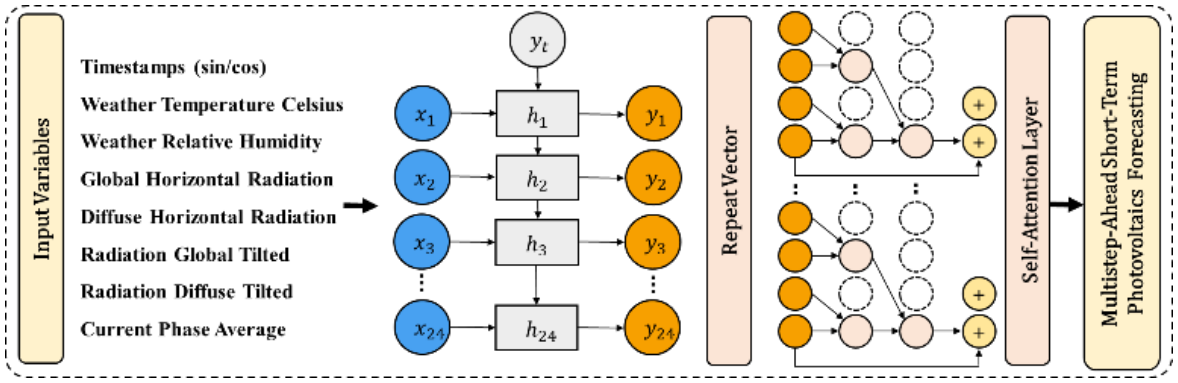

Figure 3. Example architecture of the hybrid model for multistep-ahead PV power forecasting.

The encoder in the model consists of three GRU layers with 64, 32, and 16 units, respectively. GRUs, a variant of RNNs, are computationally efficient and capable of handling long-term

 doi:10.20944/preprints202412.0711.v1

dependencies, outperforming traditional LSTMs in terms of simplicity and speed. The final GRU output serves as input to the TCN layer in the decoder. TCNs, derived from CNNs, use dilated convolutions to address long-term dependencies, excelling at capturing patterns in extended sequences. The TCN decoder employs three convolutional layers with multiple kernels, with the output processed through a GlobalAveragePooling1D layer. A self-attention mechanism is then applied to the decoder output to highlight critical time steps for forecasting.

The model's activation function is a pivotal component that influences its performance. In this study, three activation functions—ReLU, SELU, and Leaky ReLU—were evaluated. ReLU, while simple, suffers from the "dying ReLU" problem, where neurons become inactive. SELU, with its self-normalizing properties, maintains a non-zero mean and fixed variance, improving convergence and preventing vanishing gradients. Leaky ReLU mitigates the "dying ReLU" issue by allowing a small positive slope for negative values but is still susceptible to vanishing gradients in some cases. Based on these evaluations, SELU was selected as the activation function for its superior performance and stability in handling long-term dependencies.

The hybrid model adopts a many-to-many sequence-to-sequence forecasting approach to predict solar irradiance for Jeju Island and PV power for Alice Springs over the next 24 hours. The GRU encoder captures short-term temporal dependencies, while the TCN decoder identifies large-scale temporal patterns through its convolutional structure. A "repeat vector" function replicates the GRU encoder output for the 24-hour forecasting window, providing input to the TCN decoder, which generates predictions for each hour. A final dense layer refines the output, ensuring a single-dimension prediction that aligns precisely with the 24-hour forecasting horizon for enhanced accuracy and consistency.

In the case of solar irradiance forecasting, the model predicts the next 11 time points based on meteorological input variables such as temperature, humidity, wind speed, and sky condition. For PV power forecasting in Alice Springs, the model predicts hourly PV power output for the next day, leveraging multistep-ahead forecasting to support stable grid operation. This multistep approach ensures that the model not only predicts individual time steps but also captures cumulative temporal dependencies, allowing it to adapt to dynamic weather patterns and optimize forecasting accuracy. This approach captures cumulative temporal dependencies, enhancing accuracy and robustness in renewable energy forecasting.

4. Results

4.1. Experimental Design

The study evaluated the performance of the proposed hybrid DL model using two solar irradiance datasets collected from Jeju Island's Ildo-1 dong and Gosan-ri regions, as well as the DKASC dataset from Alice Springs, Australia. For the Jeju datasets, data spanning 2011 to 2018 were divided into a training set (75%) and a test set (25%). The training set included data from 2011 to 2016, while the test set covered 2017 to 2018, ensuring sufficient training data and robust testing on unseen data to evaluate the model's generalization capabilities. Similarly, the DKASC dataset was split into a 2:1 ratio, with samples consisting of 24 consecutive hours of input variables and corresponding labels for multistep-ahead forecasting.

The proposed model, integrating GRU, TCN, and self-attention mechanisms, was implemented using Python (version 3.8) with TensorFlow (version 2.9.0) and Keras (version 2.9.0), with hyperparameter settings detailed in Table 3. Training involved 50 epochs, a batch size of 24, and the SELU activation function, which was chosen for its superior self-normalizing properties and ability to handle long-term dependencies. The Huber loss function and Adam optimizer were used to ensure effective learning and minimize overfitting. Early stopping with a patience of 10 epochs was applied to improve training efficiency. These settings balanced model performance and training efficiency while avoiding overfitting.

 doi:10.20944/preprints202412.0711.v1

Table 3. Hyperparameter configuration for model training.

No.	Hyperparameter	Setting
1	Epochs	25
2	Batch size	24
3	Optimizer	Adam
4	Metrics	MAE
5	Learning rate	0.001
6	Activation function	SELU
7	Loss	Huber loss
8	Random state	42
9	Early stopping	10

To evaluate the performance of the proposed model, mean absolute error (MAE) and root mean square error (RMSE) metrics were used, as defined by Equations (9) and (10):

$$MAE = 1/n \times \sum |F_t - A_t|, \quad (9)$$

$$RMSE = (\sqrt{(\sum (F_t - A_t)^2)}/n, \quad (10)$$

where A_t and F_t represent the actual and forecasted values at time t, and n indicates the number of observations. These metrics quantify the difference between the predicted and actual values. The MAE measures the average absolute difference between the predicted and actual values. In contrast, the RMSE measures the square root of the average squared difference between the predicted and actual values.

4.2. Experimental Results

To evaluate the effectiveness of activation functions in solar irradiance prediction, the hybrid GRU-TCN model was tested using three different activation functions—ReLU, SELU, and Leaky ReLU—across two regions, Ildo-1 dong and Gosan-ri. Activation functions were chosen as a focus of analysis due to their critical role in enabling the model to learn complex patterns and dependencies in solar irradiance data. The results, summarized in Table 4, highlight significant differences in performance metrics such as MAE and RMSE, emphasizing the importance of selecting an appropriate activation function to optimize prediction accuracy and stability.

SELU achieved the lowest average MAE and RMSE values in both regions, demonstrating its ability to stabilize the learning process through its self-normalizing property. In contrast, ReLU and Leaky ReLU showed mixed performance, with ReLU performing better in some steps and Leaky ReLU showing slight improvements in others. For instance, in Ildo-1 dong, SELU achieved an average RMSE of 0.369, outperforming ReLU (0.372) and Leaky ReLU (0.387). Similarly, in Gosan-ri, SELU reduced the average RMSE to 0.496, compared to 0.501 for both ReLU and Leaky ReLU.

Table 4. Performance comparison of activation functions for solar irradiance prediction using GRU-TCN model (units: MJ/m²).

Steps	Ildo-1 dong						Gosan-ri					
	ReLU		SELU		Leaky ReLU		ReLU		SELU		Leaky ReLU	
	MAE	RMSE	MAE	RMSE	MAE	RMSE	MAE	RMSE	MAE	RMSE	MAE	RMSE
1	0.366	0.253	0.394	0.279	0.384	0.268	0.252	0.347	0.231	0.336	0.252	0.347
2	0.453	0.312	0.459	0.323	0.463	0.321	0.293	0.405	0.283	0.411	0.293	0.405
3	0.497	0.341	0.498	0.349	0.508	0.350	0.322	0.452	0.310	0.450	0.322	0.452

 doi:10.20944/preprints202412.0711.v1

4	0.525	0.359	0.526	0.365	0.539	0.370	0.346	0.484	0.333	0.483	0.346	0.484
5	0.543	0.370	0.543	0.374	0.565	0.388	0.359	0.504	0.350	0.509	0.359	0.504
6	0.556	0.380	0.556	0.379	0.587	0.400	0.369	0.518	0.361	0.524	0.369	0.518
7	0.567	0.390	0.564	0.384	0.601	0.410	0.379	0.531	0.367	0.532	0.379	0.531
8	0.581	0.403	0.571	0.390	0.612	0.420	0.390	0.546	0.374	0.540	0.390	0.546
9	0.596	0.416	0.577	0.396	0.623	0.433	0.404	0.561	0.384	0.548	0.404	0.561
10	0.612	0.429	0.588	0.407	0.633	0.444	0.420	0.579	0.394	0.558	0.420	0.579
11	0.629	0.442	0.601	0.418	0.644	0.457	0.421	0.584	0.402	0.568	0.421	0.584
Avg.	0.539	0.372	0.534	0.369	0.560	0.387	0.360	0.501	0.344	0.496	0.360	0.501

Across individual steps, SELU consistently demonstrated lower error margins, especially in the later steps where long-term dependencies became more critical. This trend underscores SELU's ability to effectively handle the cyclical nature of solar irradiance data, which requires maintaining stability and precision over extended sequences. The comparison indicates that SELU not only performs better on average but also exhibits consistent improvements across both datasets. Its ability to mitigate vanishing gradients and handle long-term dependencies makes it a preferred choice for time-series data.

Building on the analysis of activation functions, the hybrid GRU-TCN model was further compared with two benchmark models, LSTM-TCN and Bi-LSTM-TCN, to assess its relative performance and robustness in PV power forecasting. Such comparisons are critical for validating the proposed model's ability to outperform established architectures, particularly in capturing the complex temporal dependencies and nonlinear patterns inherent in PV power generation. Table 5 presents the performance metrics for the next 24-hour predictions using the DKASC Sanyo solar panel dataset, highlighting the effectiveness of the hybrid GRU-TCN model in achieving superior forecasting accuracy.

The GRU-TCN model achieved the lowest average MSE (1.970) and RMSE (3.882), outperforming the benchmark models LSTM-TCN (MSE: 1.987, RMSE: 3.950) and Bi-LSTM-TCN (MSE: 1.982, RMSE: 3.928). These improvements were particularly noticeable in the middle time steps, where the GRU-TCN model consistently exhibited lower errors, effectively balancing short-term and long-term temporal dependencies. For instance, at Step 11, the GRU-TCN model recorded an MSE of 1.923, outperforming both Bi-LSTM-TCN (1.974) and LSTM-TCN (1.930), underscoring its superior capability to learn complex patterns and maintain accuracy across the forecasting horizon.

Table 5. Performance comparison of hybrid models for PV power forecasting using Sanyo Solar Panel dataset (Units: kW).

Steps	**MSE**			**RMSE**		
	LSTM-TCN	**Bi-LSTM-TCN**	**GRU-TCN (Ours)**	**LSTM-TCN**	**Bi-LSTM-TCN**	**GRU-TCN (Ours)**
1	1.985	1.979	2.000	3.940	3.915	4.000
2	2.002	2.013	1.979	4.007	4.051	3.915
3	1.997	2.002	1.917	3.988	4.009	3.677
4	2.016	2.002	1.941	4.063	4.010	3.768
5	2.031	1.998	1.943	4.124	3.993	3.776
6	2.038	1.985	1.927	4.152	3.939	3.714
7	2.007	1.967	1.920	4.029	3.867	3.688
8	1.989	1.964	1.919	3.955	3.856	3.683
9	1.970	1.974	1.923	3.883	3.895	3.697
10	1.949	1.977	1.930	3.800	3.910	3.726
11	1.930	1.974	1.923	3.724	3.897	3.698
12	1.931	1.970	1.922	3.728	3.882	3.695

 doi:10.20944/preprints202412.0711.v1

13	1.926	1.968	1.965	3.711	3.873	3.862
14	1.952	1.974	2.007	3.811	3.898	4.027
15	1.968	1.981	2.014	3.872	3.925	4.056
16	2.002	1.967	2.031	4.010	3.870	4.124
17	1.990	1.970	2.029	3.961	3.879	4.119
18	2.013	1.975	2.026	4.051	3.900	4.105
19	2.036	1.979	2.035	4.147	3.917	4.143
20	2.029	1.984	2.001	4.115	3.937	4.004
21	2.004	1.991	1.999	4.016	3.964	3.996
22	1.996	1.995	1.967	3.984	3.981	3.867
23	1.965	1.988	1.975	3.860	3.954	3.901
24	1.970	1.985	1.979	3.880	3.939	3.916
Avg.	1.987	1.982	1.970	3.950	3.928	3.882

Notably, the GRU-TCN model's combination of GRU's efficiency in capturing short-term dependencies and TCN's strength in identifying long-range temporal patterns proved to be a significant advantage. Furthermore, the self-attention mechanism allowed the model to emphasize critical time steps, improving its focus on relevant features and ensuring higher accuracy. The comparison also highlights the GRU-TCN model's stability in multistep-ahead forecasting tasks. While both benchmark models exhibited higher variability across time steps, the GRU-TCN consistently minimized errors, demonstrating its robustness and scalability for diverse time-series forecasting applications.

5. Conclusions

This study introduced a hybrid DL model combining GRUs, TCNs, and the SELU activation function to improve the accuracy and robustness of solar irradiance and PV power forecasting. The model effectively addresses nonlinear dependencies and long-term temporal patterns in time-series data by leveraging GRUs for short-term dependency capture, TCNs for modeling extended temporal patterns, and self-attention mechanisms for identifying critical features. Evaluation results confirmed SELU as the most effective activation function, particularly for datasets with significant variability in solar irradiance, due to its self-normalizing properties that enhance stability and training efficiency.

The proposed model demonstrated superior performance in both solar irradiance and PV power forecasting tasks. For solar irradiance prediction, SELU consistently outperformed other activation functions, underscoring the importance of selecting suitable activation functions to handle cyclical meteorological data. In PV power forecasting, the GRU-TCN-SELU model surpassed benchmark models, including LSTM-TCN and Bi-LSTM-TCN, achieving an average RMSE of 1.970 and MSE of 3.882. These results validate the model's ability to balance short-term and long-term temporal dependencies while maintaining high predictive accuracy, making it a robust tool for renewable energy forecasting.

Beyond performance metrics, the proposed model offers scalability and integration potential within broader renewable energy systems. Its adaptability to diverse meteorological conditions and compatibility with smart grid systems highlight its potential for real-world energy management applications. By aligning with sustainable urban development goals, the model bridges the gap between advanced DL techniques and practical energy optimization, contributing to intelligent decision-making frameworks in smart cities.

Future research will focus on optimizing the model by exploring additional architectures and activation functions to better capture the nonlinear characteristics of renewable energy data. Incorporating more meteorological variables and testing on datasets from diverse climates will enhance its generalizability and robustness. Integrating the model into smart grids and energy storage systems can improve energy management efficiency and mitigate renewable energy intermittency. Additionally, applying the model within digital twin frameworks for smart cities can further advance intelligent energy management technologies.

In conclusion, the hybrid GRU-TCN-SELU model presents a scalable and reliable solution for solar irradiance and PV power forecasting. Its demonstrated effectiveness across diverse forecasting tasks

 doi:10.20944/preprints202412.0711.v1

underscores its potential for broader adoption in renewable energy management systems. Future work will expand experiments to additional datasets, such as DKASC, to validate the model's applicability across various environments, further refining its role in supporting sustainable energy systems and smart city development.

Funding: This research was funded by the Soonchunhyang University Research Fund.

Data Availability Statement: The data supporting the findings of this study are available from publicly accessible sources. The solar irradiance dataset for Jeju Island can be accessed via the Korea Meteorological Administration (KMA) as referenced in [50]. The photovoltaic power and meteorological dataset for Alice Springs are available through the Desert Knowledge Australia Solar Center (DKASC) platform, as detailed in [57]. For more information and to download the datasets, please refer to the respective sources.

Acknowledgments: The author wishes to thank Hwimyeong Ha of LG Energy Solution, Ltd. for his expert insights. His contributions were invaluable to the development and potential application of the technology discussed in this paper.

Conflicts of Interest: The authors declare no conflicts of interest.

References

1. Noh, B.; Ka, D.; Lee, D.; Yeo, H. Vision-based Potential Pedestrian Risk Analysis on Unsignalized Crosswalk Using Data Mining Techniques. *Appl. Sci.* **2020**, *10*, 102975. https://doi.org/10.3390/app10031057.
2. Noh, B.; Yeo, H. SafetyCube: Framework for Potential Pedestrian Risk Analysis Using Multi-Dimensional OLAP. *Accid. Anal. Prev.* **2021**, *155*, 106104. https://doi.org/10.1016/j.aap.2021.106104.
3. Noh, B.; Ka, D.; No, W.; Yeo, H. Automated Object Behavioral Feature Extraction for Potential Risk Analysis Based on Video Sensor. *arXiv* **2021**, arXiv:2107.03554. https://doi.org/10.48550/arXiv.2107.03554.
4. Jin, Z.; Noh, B.; Cho, H.; Yeo, H. Deep Learning-Based Approach on Risk Estimation of Urban Traffic Accidents. In Proceedings of the 2022 IEEE 25th International Conference on Intelligent Transportation Systems (ITSC), Macau, China, 8–12 October 2022; pp. 1446–1451. https://doi.org/10.1109/ITSC55140.2022.9922246.
5. Lee, H.; Cho, H.; Noh, B.; Yeo, H. NAVIBox: Real-Time Vehicle–Pedestrian Risk Prediction System in an Edge Vision Environment. *Electronics* **2023**, *12*, 4311. https://doi.org/10.3390/electronics12204311.
6. Jin, Z.; No, W.; Noh, B. Do Enhanced School Zone Policies Improve Pedestrians' Safety? A Deep Learning-Based Case Study of Osan City, South Korea. *Cities* **2025**, *156*, 105505. https://doi.org/10.1016/j.cities.2024.105505.
7. Kim, Y.; Yeo, H.; Lim, L.; Noh, B. Integrating Visual and Community Environments in a Motorcycle Crash and Casualty Estimation. *Accid. Anal. Prev.* **2024**, *208*, 107792. https://doi.org/10.1016/j.aap.2024.107792.
8. No, W.; Noh, B.; Kim, Y. A Novel Approach for Reliable Pedestrian Trajectory Collection with Behavior-Based Trajectory Reconstruction for Urban Surveillance Systems. *Adv. Eng. Softw.* **2024**, *195*, 103687. https://doi.org/10.1016/j.advengsoft.2024.103687.
9. No, W.; Lee, D.; Noh, B.; Kim, Y. How Do Crosswalk Delays Affect Pedestrian Access in Zoning Areas? Walking Access Reduction by Signalized Crosswalks in Seoul, South Korea. *Appl. Geogr.* **2023**, *156*, 102975. https://doi.org/10.1016/j.apgeog.2023.102975.
10. Jin, Z.; Noh, B. From Prediction to Prevention: Leveraging Deep Learning in Traffic Accident Prediction Systems. *Electronics* **2023**, 12(20), 4335. https://doi.org/10.3390/electronics12204335.
11. Hwang, J.; Noh, B.; Jin, Z.; Yeo, H. Asymmetric Long-Term Graph Multi-Attention Network for Traffic Speed Prediction. In Proceedings of the 2022 IEEE 25th International Conference on Intelligent Transportation Systems (ITSC), Macau, China, 8–12 October 2022; pp. 1498–1503. https://doi.org/10.1109/ITSC55140.2022.9922130.
12. Noh, B.; Park, H.; Yeo, H. Analyzing Vehicle–Pedestrian Interactions: Combining Data Cube Structure and Predictive Collision Risk Estimation Model. *Accid. Anal. Prev.* **2022**, *165*, 106539. https://doi.org/10.1016/j.aap.2021.106539.
13. Noh, B.; Ka, D.; Lee, D.; Yeo, H. Analysis of Vehicle–Pedestrian Interactive Behaviors near Unsignalized Crosswalk. *Transp. Res. Rec.* **2021**, *2675*, 494–505. https://doi.org/10.1177/0361198121999066.
14. Noh, B.; Yeo, H. A Novel Method of Predictive Collision Risk Area Estimation for Proactive Pedestrian Accident Prevention System in Urban Surveillance Infrastructure. *Transp. Res. C* **2022**, *137*, 103570. https://doi.org/10.1016/j.trc.2022.103570.
15. Noh, B.; No, W.; Lee, D. Vision-Based Overhead Front Point Recognition of Vehicles for Traffic Safety Analysis. In Proceedings of the 2018 ACM International Joint Conference on Pervasive and Ubiquitous Computing (UbiComp '18), Singapore, 8–12 October 2018; pp. 1096–1102. https://doi.org/10.1145/3267305.3274165.

16. Noh, B.; Cha, K.; Chang, S. Movement Classification Based on Acceleration Spectrogram with Dynamic Time Warping Method. In Proceedings of the 2017 18th IEEE International Conference on Mobile Data Management (MDM), Daejeon, Korea, 29 May–1 June 2017; pp. 397–400. https://doi.org/10.1109/MDM.2017.72.
17. Park, H.; Park, D.Y.; Noh, B.; Chang, S. Stacking Deep Transfer Learning for Short-Term Cross Building Energy Prediction with Different Seasonality and Occupant Schedule. *Build. Environ.* **2022**, *218*, 109060. https://doi.org/10.1016/j.buildenv.2022.109060.
18. Son, J.J.; Noh, B.; Park, H.; Chang, S. Optimization of Building Material Selection for Energy Saving in Commercial Buildings in Different Climatic Conditions. *J. Green Build.* **2022**, *17*, 89–106. https://doi.org/10.3992/jgb.17.3.89.
19. Shon, D.; Noh, B.; Byun, N. Identification and Extracting Method of Exterior Building Information on 3D Map. *Buildings* **2022**, *12*, 452. https://doi.org/10.3390/buildings12040452.
20. Noh, B.; Son, J.; Park, H.; Chang, S. In-Depth Analysis of Energy Efficiency Related Factors in Commercial Buildings Using Data Cube and Association Rule Mining. *Sustainability* **2017**, *9*, 109060. https://doi.org/10.3390/su9112119.
21. Lee, J.; Noh, B.; Jang, S.; Park, D.; Chung, Y.; Chang, H.H. Stress Detection and Classification of Laying Hens by Sound Analysis. Asian-Australas. *J. Anim. Sci.* **2015**, *28*, 592–599. https://doi.org/10.5713/ajas.14.0654.
22. Noh, B.; Ka, D.; Lee, J.; Lee, D. Vision-Based Potential Pedestrian Risk Analysis on Unsignalized Crosswalk Using Data Mining Techniques. *Appl. Sci.* **2020**, *10*, 102975. https://doi.org/10.3390/app10031057.
23. Kim, B.; Noh, B.; Song, K. Method on Efficient Operation of Multiple Models for Vision-Based In-Flight Risky Behavior Recognition in UAM Safety and Security. *J. Adv. Transp.* **2024**, *2024*, 7113084. https://doi.org/10.1155/2024/7113084.
24. Noh, B.; Lin, T.; Lee, S.; Jeong, T. Deep Learning and Geometry Flow Vector Using Estimating Vehicle Cuboid Technology in a Monovision Environment. *Sensors* **2023**, *23*, 7504. https://doi.org/10.3390/s23177504.
25. Min, H.; Hong, S.; Song, J.; Son, B.; Noh, B.; Moon, J. SolarFlux Predictor: A Novel Deep Learning Approach for Photovoltaic Power Forecasting in South Korea. *Electronics* **2024**, *13*, 2071. https://doi.org/10.3390/electronics13112071.
26. Moon, J.; Maqsood, M.; So, D.; Baik, S.W.; Rho, S.; Nam, Y. Advancing ensemble learning techniques for residential building electricity consumption forecasting: Insight from explainable artificial intelligence. *PLoS ONE* **2024**, *19*, e0307654. https://doi.org/10.1371/journal.pone.0307654.
27. Moon, J.; Rho, S.; Baik, S.W. Toward explainable electrical load forecasting of buildings: A comparative study of tree-based ensemble methods with Shapley values. *Sustain. Energy Technol. Assess.* **2022**, *54*, 102888. https://doi.org/10.1016/j.seta.2022.102888.
28. Moon, J.; Park, S.; Rho, S.; Hwang, E. Interpretable Short-Term Electrical Load Forecasting Scheme Using Cubist. *Comput. Intell. Neurosci.* **2022**, *2022*, 1–11. https://doi.org/10.1155/2022/6892995.
29. Oh, J.; Lee, J.; Kim, D.; Kim, B.-Y.; Moon, J. A Comparative Study on Data Augmentation Using Generative Models for Robust Solar Irradiance Prediction. *J. Korea Comput. Inf. Soc.* **2023**, *28*, 29–42. https://doi.org/10.9708/jksci.2023.28.11.029.
30. Moon, J.; Park, S.; Jung, S.; Rew, J.; Rho, S.; Hwang, E. Combination of short-term load forecasting models based on a stacking ensemble approach. *Energy Build.* **2020**, *216*, 109921. https://doi.org/10.1016/j.enbuild.2020.109921.
31. Moon, J.; Kim, J.; Kang, P.; Hwang, E. Solving the Cold-Start Problem in Short-Term Load Forecasting Using Tree-Based Methods. *Energies* **2020**, *13*, 886. https://doi.org/10.3390/en13040886.
32. Moon, J.; Park, S.; Rho, S.; Hwang, E. A comparative analysis of artificial neural network architectures for building energy consumption forecasting. *Int. J. Distrib. Sens. Netw.* **2019**, *15*, 1550147719877616. https://doi.org/10.1177/1550147719877616.
33. Moon, J.; Kim, Y.; Son, M.; Hwang, E. Hybrid Short-Term Load Forecasting Scheme Using Random Forest and Multilayer Perceptron. *Energies* **2018**, *11*, 3283. https://doi.org/10.3390/en11123283.
34. Moon, J.; Park, J.; Hwang, E.; Jun, S. Forecasting power consumption for higher educational institutions based on machine learning. *J. Supercomput.* **2018**, *74*, 3778–3800. https://doi.org/10.1007/s11227-017-2022-x.
35. Moon, J.; Kim, K.H.; Kim, Y.; Hwang, E. A Short-Term Electric Load Forecasting Scheme Using 2-Stage Predictive Analytics. In Proceedings of the 2018 IEEE International Conference on Big Data and Smart Computing (BigComp), Shanghai, China, 15–17 January 2018; pp. 219–226. https://doi.org/10.1109/BigComp.2018.00040.
36. Oh, J.; So, D.; Jo, J.; Kang, N.; Hwang, E.; Moon, J. Two-Stage Neural Network Optimization for Robust Solar Photovoltaic Forecasting. *Electronics* **2024**, *13*, 1659. https://doi.org/10.3390/electronics13091659.
37. So, D.; Oh, J.; Jeon, I.; Moon, J.; Lee, M.; Rho, S. BiGTA-Net: A Hybrid Deep Learning-Based Electrical Energy Forecasting Model for Building Energy Management Systems. *Systems* **2023**, *11*, 456. https://doi.org/10.3390/systems11090456.

38. Moon, J.; Kim, Y.; Rho, S. User Behavior Analytics with Machine Learning for Household Electricity Demand Forecasting. In Proceedings of the 2022 International Conference on Platform Technology and Service (PlatCon), Jeju, Korea, 7–9 February 2022; pp. 13–18. https://doi.org/10.1109/PlatCon55845.2022.9932037.
39. Moon, J.; Park, S.; Rho, S.; Hwang, E. Robust building energy consumption forecasting using an online learning approach with R ranger. *J. Build. Eng.* **2022**, *47*, 103851. https://doi.org/10.1016/j.jobe.2021.103851.
40. Moon, J.; Park, S.; Jung, S.; Hwang, E.; Rho, S. Training-Data Generation and Incremental Testing for Daily Peak Load Forecasting. In Proceedings of the 22nd International Conference on Artificial Intelligence (ICAI'20) and the 4th International Conference on Applied Cognitive Computing (ACC'20), Las Vegas, NV, USA, 27–30 July 2020; pp. 801–812. https://doi.org/10.1007/978-3-030-70296-0_59.
41. Gul, M.J.; Urfa, G.M.; Paul, A.; Moon, J.; Rho, S.; Hwang, E. Mid-term electricity load prediction using CNN and Bi-LSTM. *J. Supercomput.* **2021**, *77*, 10942–10958. https://doi.org/10.1007/s11227-021-03686-8.
42. Jung, S.; Moon, J.; Park, S.; Hwang, E. An Attention-Based Multilayer GRU Model for Multistep-Ahead Short-Term Load Forecasting. *Sensors* **2021**, *21*, 1639. https://doi.org/10.3390/s21051639.
43. Jung, S.; Moon, J.; Park, S.; Rho, S.; Baik, S.W.; Hwang, E. Bagging Ensemble of Multilayer Perceptrons for Missing Electricity Consumption Data Imputation. *Sensors* **2020**, *20*, 1772. https://doi.org/10.3390/s20061772.
44. Park, S.; Moon, J.; Jung, S.; Rho, S.; Baik, S.W.; Hwang, E. A Two-Stage Industrial Load Forecasting Scheme for Day-Ahead Combined Cooling, Heating and Power Scheduling. *Energies* **2020**, *13*, 443. https://doi.org/10.3390/en13020443.
45. Kim, J.; Moon, J.; Hwang, E.; Kang, P. Recurrent inception convolution neural network for multi short-term load forecasting. *Energy Build.* **2019**, *194*, 328–341. https://doi.org/10.1016/j.enbuild.2019.04.034.
46. Son, M.; Moon, J.; Jung, S.; Hwang, E. A Short-Term Load Forecasting Scheme Based on Auto-Encoder and Random Forest. In Proceedings of the 3rd International Conference on Applied Physics, System Science and Computers (APSAC 2018), Dubrovnik, Croatia, 26–28 September 2018; Lecture Notes in Electrical Engineering, vol. 574, pp. 255–262. https://doi.org/10.1007/978-3-030-21507-1_21.
47. Moon, J. A Multi-Step-Ahead Photovoltaic Power Forecasting Approach Using One-Dimensional Convolutional Neural Networks and Transformer. *Electronics* **2024**, *13*, 2007. https://doi.org/10.3390/electronics13112007.
48. Moon, J.; Han, Y.; Chang, H.; Rho, S. Multistep-ahead solar irradiance forecasting for smart cities based on LSTM, Bi-LSTM, and GRU neural networks. *J. Soc. e-Bus. Stud.* **2022**, *27*, 27–52. https://doi.org/10.7838/jsebs.2022.27.4.027.
49. Yang, T.; Kim, M.; Moon, J. Understanding Solar Irradiance Predictions Through Explainable AI: Perspectives from Gwangju. *J. Platform Technol.* **2024**, *12*, 3–16. http://doi.org/10.23023/JPT.2024.12.5.003.
50. So, D.; Oh, J.; Leem, S.; Ha, H.; Moon, J. A Hybrid Ensemble Model for Solar Irradiance Forecasting: Advancing Digital Models for Smart Island Realization. *Electronics* **2023**, *12*, 2607. https://doi.org/10.3390/electronics12122607.
51. Jang, J.; Jeong, W.; Kim, S.; Lee, B.; Lee, M.; Moon, J. RAID: Robust and interpretable daily peak load forecasting via multiple deep neural networks and Shapley values. *Sustainability* **2023**, *15*, 6951. https://doi.org/10.3390/su15086951.
52. Hussain, T.; Ullah, F.U.M.; Muhammad, K.; Rho, S.; Ullah, A.; Hwang, E.; Moon, J.; Baik, S.W. Smart and intelligent energy monitoring systems: A comprehensive literature survey and future research guidelines. *Int. J. Energy Res.* **2021**, *45*, 3590–3614. https://doi.org/10.1002/er.6093.
53. Moon, J.; Park, S.; Hwang, E.; Rho, S. A Hybrid Tree-Based Ensemble Learning Model for Day-Ahead Peak Load Forecasting. In Proceedings of the 2022 15th International Conference on Human System Interaction (HSI), Melbourne, Australia, 28–30 June 2022; pp. 1–6. https://doi.org/10.1109/HSI55341.2022.9869440.
54. Moon, J.; Shin, Z.; Rho, S.; Hwang, E. A Comparative Analysis of Tree-Based Models for Day-Ahead Solar Irradiance Forecasting. In Proceedings of the 2021 International Conference on Platform Technology and Service (PlatCon), Jeju, Korea, 13–15 February 2021; pp. 1–6. https://doi.org/10.1109/PlatCon53246.2021.9680748.
55. Park, J.; Moon, J.; Jung, S.; Hwang, E. Multistep-Ahead Solar Radiation Forecasting Scheme Based on the Light Gradient Boosting Machine: A Case Study of Jeju Island. *Remote Sens.* **2020**, *12*, 2271. https://doi.org/10.3390/rs12142271.
56. Park, S.; Moon, J.; Hwang, E. 2-Stage Electric Load Forecasting Scheme for Day-Ahead CCHP Scheduling. In Proceedings of the 2019 IEEE 13th International Conference on Power Electronics and Drive Systems (PEDS), Toulouse, France, 9–12 July 2019; pp. 1–4. https://doi.org/10.1109/PEDS44367.2019.8998960.
57. Desert Knowledge Australia Solar Centre. Available online: https://dkasolarcentre.com.au/download?location=alice-springs (accessed on 6 December 2024).

 doi:10.20944/preprints202412.0711.v1

disclaim responsibility for any injury to people or property resulting from any ideas, methods, instructions or products referred to in the content.